FRONTIERS OF PHYSICS

RESEARCH ARTICLE
Volume 19 / Issue 5 / 51201 / 2024

Quantum secure direct communication with hybrid entanglement

Peng Zhao[1,2], Wei Zhong[2], Ming-Ming Du[1], Xi-Yun Li[3], Lan Zhou[3], Yu-Bo Sheng[1,2,†]

1 College of Electronic and Optical Engineering & College of Flexible Electronics (Future Technology), Nanjing University of Posts and Telecommunications, Nanjing 210023, China
2 Institute of Quantum Information and Technology, Nanjing University of Posts and Telecommunications, Nanjing 210003, China
3 College of Science, Nanjing University of Posts and Telecommunications, Nanjing 210023, China
Corresponding author. E-mail: †shengyb@njupt.edu.cn
Received November 29, 2023; accepted January 11, 2024

ABSTRACT

Quantum secure direct communication (QSDC) can transmit secret messages without keys, making it an important branch of quantum communication. We present a hybrid entanglement-based quantum secure direct communication (HE-QSDC) protocol with simple linear optical elements, combining the benefits of both continuous variables (CV) and discrete variables (DV) encoding. We analyze the security and find that the QSDC protocol has a positive security capacity when the bit error rate is less than 0.073. Compared with previous DV QSDC protocols, our protocol has higher communication efficiency due to performing nearly deterministic Bell-state measurement. On the other hand, compared with CV QSDC protocol, this protocol has higher fidelity with large α. Based on these advantages, our protocol may provide an alternative approach to realize secure communication.

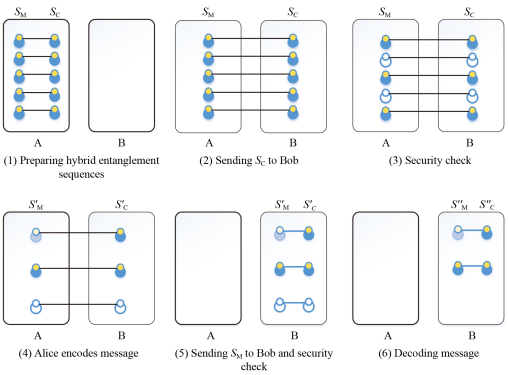

Quantum secure direct communication with hybrid entanglement

Keywords quantum secure direct communication, hybrid entanglement, Bell-state measurement

1 Introduction

Quantum communication refers to the realization of information transmission based on the basic principles of quantum mechanics, which has been widely concerned because of its theoretical unconditional security [1, 2]. Quantum key distribution (QKD) provides an unconditionally secure means of distributing secret keys between two spatially separated parties [3–6]. Quantum secret sharing (QSS) [7, 8] uses quantum channels to share random keys among multiple parties. Both QKD and QSS do not transmit the message directly. Besides QKD and QSS, there is another important quantum communication branch, named quantum secure direct communication (QSDC) [9–11]. Different from QKD and QSS, QSDC enables secret information to be transmitted directly through a quantum channel without neither key nor ciphertext. Long and Liu [9] introduced the first QSDC protocol. In 2003, the two-step QSDC protocol was proposed [10]. In this protocol, they transmit the Einstein–Podolsky–Rosen (EPR) pairs in two steps with security checking applied in each step to avoid the leakage of information. Recently, QSDC was developed in both theory and experiments. For example, in theory, the measurement-device-independent (MDI) QSDC [12, 13], device-independent (DI) QSDC [14–16], one-step QSDC protocols [17–19], and some other important QSDC protocols were proposed [20–30]. In experiment, in 2016, the first QSDC experiment using single photon was realized [31]. In 2017, with the help of quantum memory (QM), the first entanglement-based QSDC protocol was realized [32]. In the same year, the QSDC experiment using 500 m optical fiber was realized [33]. The QSDC experiment in free-space was reported in 2020 [34]. In 2021,

https://doi.org/10.1007/s11467-024-1396-5

the first QSDC network was realized [35]. In 2022, fiber-based QSDC without active polarization compensation was reported [36]. The distance of QSDC reached 100 km in 2022 [37]. Recently, an interesting QSDC experiment using squeezed state was realized [38].

In quantum communication, photons are frequently used to transmit information due to its rapidity of transmission. Two different ways of encoding, i.e., discrete variable (DV) and continuous variable (CV) are used. In DV regime, for a single photon, the polarization degree of freedom (DOF) is usually used to encode the information for its simple manipulation [39–41]. In the CV regime, the carrier of information is the regular component of the light field states (position and momentum in phase space) rather than the DOFs (such as polarization and phase) of the photon. A great number of important works on both DV encoding [42–44] and CV encoding [45–48] have been reported and they have made considerable progress in recent decades. In QSDC, the QSDC protocols using DV encoding [9–15, 17–20, 24] and CV encoding [25–27] are also proposed independently.

However, both DV and CV have their own advantages and disadvantages [49, 50]. For example, in DV encoding, it is difficulty to implement a deterministic two-bit controlled gate operation [51, 52]. Moreover, the Bell-state measurement (BSM) is an indispensable tool in quantum communication and the success probability of BSM is only 50% [53, 54]. On the other hand, the characteristics and advantages of CV entanglement, such as coherent state entanglement [55], lies in its ability to achieve near-deterministic BSM, high-efficiency detections, and unconditional operations [56]. The coherent-state Bell state measurements have been employed in both twin-field QKD (TF-QKD) [57] and device-independent QKD (DI-QKD) [58], which not only enhances the secure transmission distance but also ensures the security of the measurement device independence and device independence. However, achieving high efficiencies and unconditional operations often come at the cost of lower fidelity and this approach generally introduces losses [59].

A novel type of hybrid entanglement coding that combines the advantages of CV and DV has been proposed and realized [60–62]. Especially the hybrid entanglement based on coherent-state and polarized photons received the attention of researchers [63–65]. Many interesting protocols using hybrid systems have been proposed, such as hybrid quantum repeater [66, 67], hybrid entanglement QKD [68–72], hybrid entanglement purification [73], and some other interesting protocols [74, 75].

In this paper, we present the first hybrid entanglement-based QSDC (HE-QSDC) protocol. The hybrid qubit can be described as $|0_{\rm L}\rangle = |+\rangle|\alpha\rangle, |1_{\rm L}\rangle = |-\rangle|-\alpha\rangle$, where $|\pm\rangle = \frac{1}{\sqrt{2}}(|H\rangle \pm |V\rangle)$ and the subscript L represents the logical qubit. Here, $|H\rangle$ and $|V\rangle$ denote the horizontal and vertical polarization modes of photons, respectively. $|\alpha\rangle$ is the coherent state. Compared to existing DV QSDC protocols, our protocol has a higher communication efficiency due to the use of near-deterministic BSM. Additionally, for QSDC protocols that rely on CV entanglement, we have shown that our protocol has a higher fidelity when satisfying the large α required for near-deterministic BSM.

The structure of this paper is organized as follows. In Section 2, we first describe the hybrid qubits and the key element of this protocol, i.e., near-deterministic BSM. In Section 3, we propose the HE-QSDC protocol subsequently. In Section 4, we analyze the security of our HE-QSDC protocol. In Section 5, we analyze the fidelities of hybrid entanglement and CV entanglement in a lossy environment. In Section 6, we perform a discussion and conclusion.

2 Hybrid Bell states measurement

In this section, we briefly introduce the hybrid Bell states measurement (HBSM). The hybrid Bell states can be written as follows:

$$|\Phi^{\pm}\rangle = \frac{1}{\sqrt{2}}(|0_{\rm L}0_{\rm L}\rangle \pm |1_{\rm L}1_{\rm L}\rangle),$$
$$|\Psi^{\pm}\rangle = \frac{1}{\sqrt{2}}(|0_{\rm L}1_{\rm L}\rangle \pm |1_{\rm L}0_{\rm L}\rangle). \quad (1)$$

In Ref. [51], a method was proposed and implemented to convert between the four hybrid Bell states using the Pauli X and Z operations. This demonstrates that it is possible to transform one Bell states into another using these operations. Before introducing the BSM, it is helpful to briefly review the two existing types of BSMs: the coherent-state BSM and polarized-state BSM. The four entangled coherent Bell states, represented as $|\phi^{\pm}\rangle_C = \frac{1}{C_{\pm}}(|\alpha\rangle|\alpha\rangle \pm |-\alpha\rangle|-\alpha\rangle)$ and $|\psi^{\pm}\rangle_C = \frac{1}{C_{\pm}}(|\alpha\rangle|-\alpha\rangle \pm |-\alpha\rangle|\alpha\rangle)$, can be distinguished using a coherent-state BSM, which involves a 50:50 beam splitter (BS) and two photon number parity detectors (PNPDs) [76]. Here, $\frac{1}{C_{\pm}} = \frac{1}{\sqrt{2\pm 2e^{-4|\alpha|^2}}}$ represent the normalization constants. The setup is shown in Fig. 1 (M1) [51], with the subscript C denoting the coherent state. After passing through the BS, the four coherent Bell states can be transformed into the states as

$$|\phi^{+}\rangle_C = \frac{1}{C_{+}}(|\alpha\rangle|\alpha\rangle + |-\alpha\rangle|-\alpha\rangle) \xrightarrow{BS} |even\rangle|0\rangle,$$
$$|\phi^{-}\rangle_C = \frac{1}{C_{-}}(|\alpha\rangle|\alpha\rangle - |-\alpha\rangle|-\alpha\rangle) \xrightarrow{BS} |odd\rangle|0\rangle,$$
$$|\psi^{+}\rangle_C = \frac{1}{C_{+}}(|\alpha\rangle|-\alpha\rangle + |-\alpha\rangle|\alpha\rangle) \xrightarrow{BS} |0\rangle|even\rangle,$$
$$|\psi^{-}\rangle_C = \frac{1}{C_{-}}(|\alpha\rangle|-\alpha\rangle - |-\alpha\rangle|\alpha\rangle) \xrightarrow{BS} |0\rangle|odd\rangle. \quad (2)$$

Here, $|even\rangle = \frac{1}{C_{+}}(|\sqrt{2}\alpha\rangle + |-\sqrt{2}\alpha\rangle)$ with the normalization constant of $\frac{1}{C_{+}}$ and $|odd\rangle = \frac{1}{C_{-}}(|\sqrt{2}\alpha\rangle - |-\sqrt{2}\alpha\rangle)$ with the normalization constant of $\frac{1}{C_{-}}$ contain only even and odd

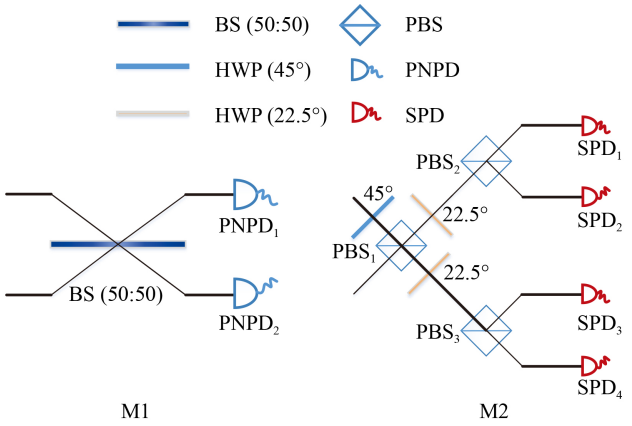

Fig. 1 Two Bell states measurement (BSM) elements in our protocol [51]. M1 is coherent state BSM element implemented by 50:50 beam splitter (BS) and two photon number parity detectors (PNPDs). It can unambiguously distinguish all four coherent Bell states with a high success rate $1-\mathrm{e}^{-2|\alpha|^2}$. The measurement fails only when no photon is detected at both PNPDs. M2 is BSM for polarized state with 50% success probability to discriminate two states $|\psi_P^{\pm}\rangle = |H\rangle|V\rangle \pm |V\rangle|H\rangle$. This measurement succeeds only when one detector from the upper two and another from the lower two detect a photon simultaneously.

photon number states, respectively. Therefore, the four coherent Bell states can be discriminated by parity measurements of the photons at the output. However, there is a possibility of failure when no photon is detected at both the PNPDs. This may imply that the coherent Bell state is $|\phi^+\rangle_C$ or $|\psi^+\rangle_C$ with an even output of zero.

Figure 1 (M2) shows a feasible approach for implementing a polarized-state BSM, using single photon detectors (SPDs), polarization beam splitters (PBSs), and half wave plates (HWPs). The subscript P indicates the polarized-state. In this protocol, two Bell states $|\psi^{\pm}\rangle_P = \frac{1}{\sqrt{2}}(|H\rangle|V\rangle \pm |V\rangle|H\rangle)$ can be identified only when one detector from the upper two and another detector from the lower two register a photon at the same time, with a success probability of 1/2.

The hybrid Bell states, as shown in Eq. (1), can be discriminated near-deterministically by combining linear optics with M1 and M2 [51]. Therefore, we can extend Eq. (1) and express the hybrid Bell states in terms of the standard form as follows:

$$\begin{aligned}
|\Phi^{\pm}\rangle &= \frac{1}{\sqrt{2}}(|0_{\mathrm{L}}0_{\mathrm{L}}\rangle \pm |1_{\mathrm{L}}1_{\mathrm{L}}\rangle) \\
&= \frac{1}{\sqrt{2}}(|\phi^+\rangle_P|\phi^{\pm}\rangle_C + |\psi^+\rangle_P|\phi^{\mp}\rangle_C), \\
|\Psi^{\pm}\rangle &= \frac{1}{\sqrt{2}}(|0_{\mathrm{L}}1_{\mathrm{L}}\rangle \pm |1_{\mathrm{L}}0_{\mathrm{L}}\rangle) \\
&= \frac{1}{\sqrt{2}}(|\phi^-\rangle_P|\psi^{\pm}\rangle_C - |\psi^-\rangle_P|\psi^{\mp}\rangle_C). \qquad (3)
\end{aligned}$$

Table 1 The results for hybrid Bell states measurement (HBSM). The elements in the first row represent the four possible outcomes in the coherent BSM, while the first column stands for the two recognizable outcomes in the polarized BSM, with F_p indicating a failure. The other cells in the table represent the HBSM outcomes, which are determined by the row and column that correspond to the coherent and polarized BSM results, respectively. The asterisk denotes combinations that are not possible or indicate a failure if one occurs.

	$\|\phi^+\rangle_C$	$\|\phi^-\rangle_C$	$\|\psi^+\rangle_C$	$\|\psi^-\rangle_C$
$\|\psi^+\rangle_P$	$\|\Phi^-\rangle$	$\|\Phi^+\rangle$	*	*
$\|\psi^-\rangle_P$	*	*	$\|\Psi^-\rangle$	$\|\Psi^+\rangle$
F_p	$\|\Phi^+\rangle$	$\|\Phi^-\rangle$	$\|\Psi^+\rangle$	$\|\Psi^-\rangle$

Here, $|\phi^{\pm}\rangle_P = \frac{1}{\sqrt{2}}(|H\rangle|H\rangle \pm |V\rangle|V\rangle)$.

Equation (3) shows that each hybrid Bell state can be decomposed into a combination of polarized Bell states and coherent Bell states. As a result, we can determine the BSM outcome of the hybrid entangled states by conducting two independent BSMs: one on the polarization state and the other on the coherent state. Table 1 provides a detailed breakdown of these two BSM outcomes, allowing us to extract the complete information about the hybrid entangled state.

Based on Table 1, the discrimination process is highly likely to succeed unless both M1 and M2 fail to perform the BSM simultaneously. The failure probability F_p in this scenario is calculated to be $\frac{1}{2}\mathrm{e}^{-2\alpha^2}$. Hence, it is possible to unambiguously distinguish the four coherent Bell states with a success probability of $1-\frac{1}{2}\mathrm{e}^{-2\alpha^2}$. Notably, the success rate increases with the value of parameter α. For instance, a success rate of 99% can be achieved by setting α to 1.4 [51].

3 Hybrid entanglement quantum secure direct communication

As pointed out in Ref. [9], the security of a two-step QSDC protocol relies on the transmission of entangled photons in blocks and the verification of their security at each step. Our proposed HE-QSDC protocol, which utilizes near-deterministic BSM, follows a similar approach to ensure its security. Figure 2 illustrates a schematic diagram of the proposed HE-QSDC protocol, while the specific steps of the protocol are outlined as follows.

Step (1): Prepare sequence. Alice prepares N hybrid entangled photon pairs as $|\Phi_{\mathrm{A}}^+\rangle = \frac{1}{\sqrt{2}}(|0_{\mathrm{L}}\rangle_{\mathrm{C}}|0_{\mathrm{L}}\rangle_{\mathrm{M}} + |1_{\mathrm{L}}\rangle_{\mathrm{C}}|1_{\mathrm{L}}\rangle_{\mathrm{M}})$. Here, the subscripts C and M mean the qubit in check sequence or message sequence.

Step (2): Transmit sequence. Alice sends a string of qubits, denoted as S_{C}, to Bob. Here we should point out

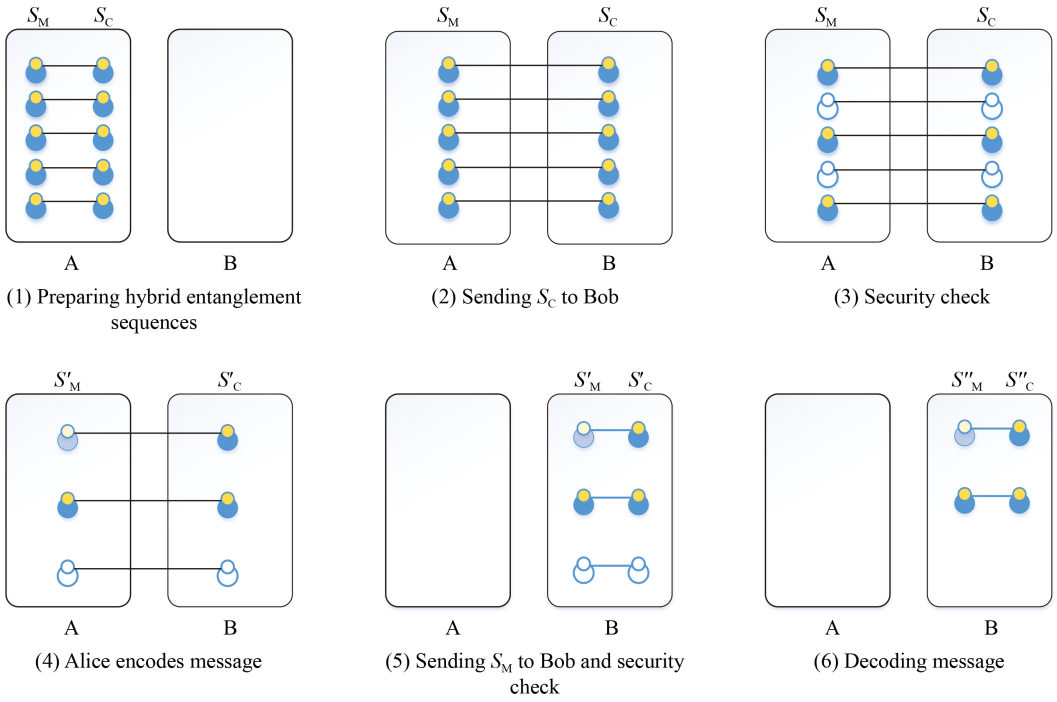

Fig. 2 Illustration for the HE-QSDC with a sequence of hybrid entangled photon pairs. The two particles that combine together represent a hybrid qubit and the two parts connected with a line are in a hybrid Bell entanglement. The smaller circles represent the polarization state and the larger circles represent the coherent state. S_M represents message sequence and S_C is check sequence.

that such transmit requires two different channels, the one is for the single photon and the other is for the coherent state. Bob selects a suitable number of photons both from two channels from S_C and performs measurements on them using one of two measurement bases randomly: the rectilinear basis Z comprised of states $Z:\{|0_L\rangle,|1_L\rangle\}$, or the diagonal basis X composed of states $X:\{\frac{1}{\sqrt{2}}(|0\rangle_L+|1\rangle_L),\frac{1}{\sqrt{2}}(|0\rangle_L-|1\rangle_L)\}$. These two basis have already been defined and used in quantum teleportation in Ref. [51]. After performing the measurements, Bob uses the classical channel to inform Alice which photons he has measured from S_C, along with the corresponding information about which measurement bases were used and the results of the measurements.

Step (3): Check security. After receiving Bob's information about the measurements from Step (2), Alice selects the corresponding photons in the message sequence and measures them using the same measurement basis as Bob. She then compares her measurement results with those reported by Bob, performing an error rate analysis to check for security breaches. If the error rate is below the preset security threshold, it can be assumed that there is no eavesdropper monitoring the quantum channel. Otherwise, the communication is terminated and both parties return to Step (1). In our hybrid encoding protocol, we use logical bit bases instead of physical bit bases for security check, which differs from the previous QSDC protocols. In a noiseless channel, Alice and Bob should obtain identical measurement results in the absence of eavesdropping. Specifically, the entangled state $|\Phi^+\rangle$ should be uniform under both the Z-basis and X-basis. Therefore, if both parties randomly select the same measurement basis, they will obtain the same measurement result. Any eavesdropping attempt will inevitably impact the entanglement between S_C and S_M, leading to different measurement results and increased error rates. The transmission of the S_C is mainly to detect the transmission security of the entangled system without encoding confidential information.

Step (4): Encode message. Under the condition of ensuring the security transmission of S_C, Alice selects one of the four unitary operations ($U_0=I$, $U_1=\sigma_z$, $U_2=\sigma_x$, $U_3=\sigma_y$) correspondingly to encode information on each quantum state in the sequence S'_M (the remaining photons after discarding the photons used for the first round of security detection in the S_M). Here, I, σ_z, σ_x and σ_y are four Pauli operators [see Eq. (4)]. The four unitary operations U_0, U_1, U_2, and U_3 can represent the information 00, 01, 10, and 11, respectively. Here

$$\begin{aligned}
U_0 &= I = |0_L\rangle\langle 0_L| + |1_L\rangle\langle 1_L|,\\
U_1 &= \sigma_z = |0_L\rangle\langle 0_L| - |1_L\rangle\langle 1_L|,\\
U_2 &= \sigma_x = |1_L\rangle\langle 0_L| + |0_L\rangle\langle 1_L|,\\
U_3 &= \sigma_y = |1_L\rangle\langle 0_L| - |0_L\rangle\langle 1_L|.
\end{aligned} \tag{4}$$

The required unitary transformations can be accomplished by utilizing a combination of Pauli X operations and Pauli Z operations. Specifically, we can implement $|+\rangle \rightleftharpoons |-\rangle$ by using a polarizing rotator on a single photon mode, and $|\alpha\rangle \rightleftharpoons |-\alpha\rangle$ by using a π phase shifter on a coherent state mode. An arbitrary Z-rotation can be implemented by applying a phase shift operation on a single photon mode ($\{+\rangle, |-\rangle\} \rightarrow \{+\rangle, \mathrm{e}^{\mathrm{i}\theta}|-\rangle\}$), without the need for any operation on a coherent state mode. Here θ is the rotation angle [51]. Alice also needs to select some photons and randomly perform one of the four unitary operations to secure the second transmission.

Step (5): Check security. After Step (4), Alice sends $S_{\mathrm{M}}^{'}$ to Bob. In order to check the transmission security of $S_{\mathrm{M}}^{'}$, Alice will tell Bob which hybrid entanglement pairs she has performed security check coding and the corresponding operations she did. Bob judges whether the second round of transmission is secure by estimating the error rate of the channel. In fact, the eavesdropper can only interfere with the transmission but cannot steal information in the second round of transmission, because he can obtain only one logic qubit from the hybrid entanglement.

Step (6): Decode message. Bob decodes the message by using the HBSM on the remaining hybrid entanglement (see Fig. 1) and reads out the message directly with Eq. (4) and Table 1. For example, the result of HBSM is $|\Psi^{+}\rangle$, the secret information is 01.

4 Security analysis of hybrid entanglement QSDC

Inspired by Refs. [77, 78], we will conduct a security analysis and calculate the security capacity of our HE-QSDC protocol in this section. To facilitate subsequent explanations, we will introduce and define some key terms,

$$\begin{aligned}
|\Phi_1\rangle &= |\Phi^{+}\rangle = \frac{1}{\sqrt{2}}(|0_{\mathrm{L}}0_{\mathrm{L}}\rangle + |1_{\mathrm{L}}1_{\mathrm{L}}\rangle),\\
|\Phi_2\rangle &= |\Phi^{-}\rangle = \frac{1}{\sqrt{2}}(|0_{\mathrm{L}}0_{\mathrm{L}}\rangle - |1_{\mathrm{L}}1_{\mathrm{L}}\rangle),\\
|\Phi_3\rangle &= |\Psi^{+}\rangle = \frac{1}{\sqrt{2}}(|0_{\mathrm{L}}1_{\mathrm{L}}\rangle + |1_{\mathrm{L}}0_{\mathrm{L}}\rangle),\\
|\Phi_4\rangle &= |\Psi^{-}\rangle = \frac{1}{\sqrt{2}}(|0_{\mathrm{L}}1_{\mathrm{L}}\rangle - |1_{\mathrm{L}}0_{\mathrm{L}}\rangle).
\end{aligned} \tag{5}$$

When Eve can obtain as much information as possible, we consider a pure state system $|\Psi_{\mathrm{ABE}}\rangle$ of ρ_{AB} as

$$\begin{aligned}
|\Psi_{\mathrm{ABE}}\rangle = \sum_{i=1}^{4}\sqrt{\lambda_i}|\Phi_i\rangle|E_i\rangle &= \sqrt{\lambda_1}|\Phi_1\rangle|E_1\rangle + \sqrt{\lambda_2}|\Phi_2\rangle\\
&\otimes |E_2\rangle + \sqrt{\lambda_3}|\Phi_3\rangle|E_3\rangle + \sqrt{\lambda_4}|\Phi_4\rangle|E_4\rangle.
\end{aligned} \tag{6}$$

Here, $|\Phi_i\rangle$ mean the Bell states of Alice and Bob and $|E_i\rangle$ represent the states of Eve's auxiliary system which are mutually orthogonal. Here

$$\rho_{\mathrm{AB}} = \lambda_1|\Phi_1\rangle\langle\Phi_1| + \lambda_2|\Phi_2\rangle\langle\Phi_2| + \lambda_3|\Phi_3\rangle\langle\Phi_3| + \lambda_4|\Phi_4\rangle\langle\Phi_4|, \tag{7}$$

where ρ_{AB} represents Alice and Bob both perform the same transformation chosen randomly from U_0, U_1, U_2, U_3. These operations will eliminate the nondiagonal elements of ρ_{AB} in Bell basis. λ_i are the probability of $|\Phi_i\rangle$. The bit and phase error rate can be expressed as $\epsilon_x = \lambda_3 + \lambda_4$ and $\epsilon_z = \lambda_2 + \lambda_4$, respectively. In this way,

$$\begin{aligned}
\rho_{\mathrm{ABE}} &= |\Psi_{\mathrm{ABE}}\rangle\langle\Psi_{\mathrm{ABE}}|\\
&= \lambda_1|\Phi_1\rangle|E_1\rangle\langle E_1|\langle\Phi_1| + \sqrt{\lambda_1\lambda_2}|\Phi_1\rangle|E_1\rangle\langle E_2|\langle\Phi_2|\\
&\quad + \sqrt{\lambda_1\lambda_3}|\Phi_1\rangle|E_1\rangle\langle E_3|\langle\Phi_3| + \sqrt{\lambda_1\lambda_4}|\Phi_1\rangle|E_1\rangle\langle E_4|\langle\Phi_4|\\
&\quad + \sqrt{\lambda_2\lambda_1}|\Phi_2\rangle|E_2\rangle\langle E_1|\langle\Phi_1| + \lambda_2|\Phi_2\rangle|E_2\rangle\langle E_2|\langle\Phi_2|\\
&\quad + \sqrt{\lambda_2\lambda_3}|\Phi_2\rangle|E_2\rangle\langle E_3|\langle\Phi_3| + \sqrt{\lambda_2\lambda_4}|\Phi_2\rangle|E_2\rangle\langle E_4|\langle\Phi_4|\\
&\quad + \sqrt{\lambda_3\lambda_1}|\Phi_3\rangle|E_3\rangle\langle E_1|\langle\Phi_1| + \sqrt{\lambda_3\lambda_2}|\Phi_3\rangle|E_3\rangle\langle E_2|\langle\Phi_2|\\
&\quad + \lambda_3|\Phi_3\rangle|E_3\rangle\langle E_3|\langle\Phi_3| + \sqrt{\lambda_3\lambda_4}|\Phi_3\rangle|E_3\rangle\langle E_4|\langle\Phi_4|\\
&\quad + \sqrt{\lambda_4\lambda_1}|\Phi_4\rangle|E_4\rangle\langle E_1|\langle\Phi_1| + \sqrt{\lambda_4\lambda_2}|\Phi_4\rangle|E_4\rangle\langle E_2|\langle\Phi_2|\\
&\quad + \sqrt{\lambda_4\lambda_3}|\Phi_4\rangle|E_4\rangle\langle E_3|\langle\Phi_3| + \lambda_4|\Phi_4\rangle|E_4\rangle\langle E_4|\langle\Phi_4|.
\end{aligned} \tag{8}$$

In order to get the maximal information, Eve intercepts all the photons and measures them in Step (5). So we trace out B from ABE, we can get

$$\begin{aligned}
Tr_B(\rho_{\mathrm{ABE}}) &= \langle 0_B|\rho|0_B\rangle + \langle 1_B|\rho|1_B\rangle\\
&= \frac{1}{2}(\lambda_1|0\rangle|E_1\rangle\langle E_1|\langle 0| + \sqrt{\lambda_1\lambda_2}|0\rangle|E_1\rangle\langle E_2|\langle 0|\\
&\quad + \sqrt{\lambda_1\lambda_3}|0\rangle|E_1\rangle\langle E_3|\langle 1| - \sqrt{\lambda_1\lambda_4}|0\rangle|E_1\rangle\langle E_4|\langle 1|\\
&\quad + \sqrt{\lambda_2\lambda_1}|0\rangle|E_2\rangle\langle E_1|\langle 0| + \lambda_2|0\rangle|E_2\rangle\langle E_2|\langle 0|\\
&\quad + \sqrt{\lambda_2\lambda_3}|0\rangle|E_2\rangle\langle E_3|\langle 1| - \sqrt{\lambda_2\lambda_4}|0\rangle|E_2\rangle\langle E_4|\langle 1|\\
&\quad + \sqrt{\lambda_3\lambda_1}|1\rangle|E_3\rangle\langle E_1|\langle 0| + \sqrt{\lambda_3\lambda_2}|1\rangle|E_3\rangle\langle E_2|\langle 0|\\
&\quad + \lambda_3|1\rangle|E_3\rangle\langle E_3|\langle 1| - \sqrt{\lambda_3\lambda_4}|1\rangle|E_3\rangle\langle E_4|\langle 1|\\
&\quad - \sqrt{\lambda_4\lambda_1}|1\rangle|E_4\rangle\langle E_1|\langle 0| - \sqrt{\lambda_4\lambda_2}|1\rangle|E_4\rangle\langle E_2|\langle 0|\\
&\quad - \sqrt{\lambda_4\lambda_3}|1\rangle|E_4\rangle\langle E_3|\langle 1| + \lambda_4|1\rangle|E_4\rangle\langle E_4|\langle 1|)\\
&\quad + \frac{1}{2}(\lambda_1|1\rangle|E_1\rangle\langle E_1|\langle 1| - \sqrt{\lambda_1\lambda_2}|1\rangle|E_1\rangle\langle E_2|\langle 1|\\
&\quad + \sqrt{\lambda_1\lambda_3}|1\rangle|E_1\rangle\langle E_3|\langle 0| + \sqrt{\lambda_1\lambda_4}|1\rangle|E_1\rangle\langle E_4|\langle 0|\\
&\quad - \sqrt{\lambda_2\lambda_1}|1\rangle|E_2\rangle\langle E_1|\langle 1| + \lambda_2|1\rangle|E_2\rangle\langle E_2|\langle 1|\\
&\quad - \sqrt{\lambda_2\lambda_3}|1\rangle|E_2\rangle\langle E_3|\langle 0| - \sqrt{\lambda_2\lambda_4}|1\rangle|E_2\rangle\langle E_4|\langle 0|\\
&\quad + \sqrt{\lambda_3\lambda_1}|0\rangle|E_3\rangle\langle E_1|\langle 1| - \sqrt{\lambda_3\lambda_2}|0\rangle|E_3\rangle\langle E_2|\langle 1|\\
&\quad + \lambda_3|0\rangle|E_3\rangle\langle E_3|\langle 0| + \sqrt{\lambda_3\lambda_4}|0\rangle|E_3\rangle\langle E_4|\langle 0|\\
&\quad + \sqrt{\lambda_4\lambda_1}|0\rangle|E_4\rangle\langle E_1|\langle 1| - \sqrt{\lambda_4\lambda_2}|0\rangle|E_4\rangle\langle E_2|\langle 1|\\
&\quad + \sqrt{\lambda_4\lambda_3}|0\rangle|E_4\rangle\langle E_3|\langle 0| + \lambda_4|0\rangle|E_4\rangle\langle E_4|\langle 0|)\\
&= \frac{1}{2}(\rho_{|\psi_1\rangle} + \rho_{|\phi_1\rangle}).
\end{aligned} \tag{9}$$

Here, $\rho_{|\psi_1\rangle}$ and $\rho_{|\phi_1\rangle}$ are the density matrix of $|\psi_1\rangle$ and $|\phi_1\rangle$,

respectively. Note that both $|0\rangle$ and $|1\rangle$ represent hybrid qubits $|0_{\rm L}\rangle$ and $|1_{\rm L}\rangle$ respectively, which we have defined above. For simplicity, we omit the subscript L here. $|\psi_1\rangle$ and $|\phi_1\rangle$ are defined as follows:

$$\begin{aligned}|\psi_1\rangle &= |0\rangle(\sqrt{\lambda_1}|E_1\rangle + \sqrt{\lambda_2}|E_2\rangle) + |1\rangle(\sqrt{\lambda_3}|E_3\rangle \\ &\quad - \sqrt{\lambda_4}|E_4\rangle),\\ |\phi_1\rangle &= |0\rangle(\sqrt{\lambda_3}|E_3\rangle + \sqrt{\lambda_4}|E_4\rangle) + |1\rangle(\sqrt{\lambda_1}|E_1\rangle \\ &\quad - \sqrt{\lambda_2}|E_2\rangle).\end{aligned} \tag{10}$$

Notice that in Step (4), Alice has applied four unitary operations U_0, U_1, U_2, and U_3 to encode message, which represent the information 00, 01, 10 and 11 respectively. So the four encoding states are defined as

$$\begin{aligned}\rho_{\rm AE,00} &= U_0\rho_{\rm AE}U_0^\dagger = \frac{1}{2}(\rho_{|\psi_1\rangle} + \rho_{|\phi_1\rangle}),\\ \rho_{\rm AE,01} &= U_1\rho_{\rm AE}U_1^\dagger = \frac{1}{2}(\rho_{\sigma_z|\psi_1\rangle} + \rho_{\sigma_z|\phi_1\rangle}),\\ \rho_{\rm AE,10} &= U_2\rho_{\rm AE}U_2^\dagger = \frac{1}{2}(\rho_{\sigma_x|\psi_1\rangle} + \rho_{\sigma_x|\phi_1\rangle}),\\ \rho_{\rm AE,11} &= U_3\rho_{\rm AE}U_3^\dagger = \frac{1}{2}(\rho_{\sigma_x\sigma_z|\psi_1\rangle} + \rho_{\sigma_x\sigma_z|\phi_1\rangle}).\end{aligned} \tag{11}$$

By exploiting Holevo bound in Refs. [77, 79], we can obtain

$$I(A:E) \le S(\sum_a p_a\rho_{{\rm AE},a}) - 1, \tag{12}$$

where $\rho_{{\rm AE},a}$ and p_a represent the encoded states and its probability distributions, respectively. Now our main task is to figure out $S(\sum_a p_a\rho_{{\rm AE},a})$, which is undoubtedly complicated work. Encouragingly, Jozsa and Schlienz [80] came up with one Gram matrix method for calculating the Von Neumann entropy of $\sum_a p_a\rho_{{\rm AE},a}$. From Eq. (11), we can get

$$\begin{aligned}|\xi_1\rangle &= I|\psi_1\rangle = \frac{1}{\sqrt{2}}[|0\rangle(\sqrt{\lambda_1}|E_1\rangle + \sqrt{\lambda_2}|E_2\rangle)\\ &\quad + |1\rangle(\sqrt{\lambda_3}|E_3\rangle - \sqrt{\lambda_4}|E_4\rangle)],\\ |\xi_2\rangle &= \sigma_z|\psi_1\rangle = \frac{1}{\sqrt{2}}[|0\rangle(\sqrt{\lambda_1}|E_1\rangle + \sqrt{\lambda_2}|E_2\rangle)\\ &\quad - |1\rangle(\sqrt{\lambda_3}|E_3\rangle - \sqrt{\lambda_4}|E_4\rangle)],\\ |\xi_3\rangle &= \sigma_x|\psi_1\rangle = \frac{1}{\sqrt{2}}[|1\rangle(\sqrt{\lambda_1}|E_1\rangle + \sqrt{\lambda_2}|E_2\rangle)\\ &\quad + |0\rangle(\sqrt{\lambda_3}|E_3\rangle - \sqrt{\lambda_4}|E_4\rangle)],\\ |\xi_4\rangle &= \sigma_x\sigma_z|\psi_1\rangle = \frac{1}{\sqrt{2}}[|1\rangle(\sqrt{\lambda_1}|E_1\rangle + \sqrt{\lambda_2}|E_2\rangle)\\ &\quad - |0\rangle(\sqrt{\lambda_3}|E_3\rangle - \sqrt{\lambda_4}|E_4\rangle)],\\ |\xi_5\rangle &= I|\phi_1\rangle = \frac{1}{\sqrt{2}}[|0\rangle(\sqrt{\lambda_3}|E_3\rangle + \sqrt{\lambda_4}|E_4\rangle)\\ &\quad + |1\rangle(\sqrt{\lambda_1}|E_1\rangle - \sqrt{\lambda_2}|E_2\rangle)],\\ |\xi_6\rangle &= \sigma_z|\phi_1\rangle = \frac{1}{\sqrt{2}}[|0\rangle(\sqrt{\lambda_3}|E_3\rangle + \sqrt{\lambda_4}|E_4\rangle)\\ &\quad - |1\rangle(\sqrt{\lambda_1}|E_1\rangle - \sqrt{\lambda_2}|E_2\rangle)],\\ |\xi_7\rangle &= \sigma_x|\phi_1\rangle = \frac{1}{\sqrt{2}}[|1\rangle(\sqrt{\lambda_3}|E_3\rangle + \sqrt{\lambda_4}|E_4\rangle)\\ &\quad + |0\rangle(\sqrt{\lambda_1}|E_1\rangle - \sqrt{\lambda_2}|E_2\rangle)],\\ |\xi_8\rangle &= \sigma_x\sigma_z|\phi_1\rangle = \frac{1}{\sqrt{2}}[|1\rangle(\sqrt{\lambda_3}|E_3\rangle + \sqrt{\lambda_4}|E_4\rangle)\\ &\quad - |0\rangle(\sqrt{\lambda_1}|E_1\rangle - \sqrt{\lambda_2}|E_2\rangle)].\end{aligned} \tag{13}$$

The Gram matrix is defined as follows:

$$G_{ij} = \sqrt{p_ip_j}\langle\xi_i|\xi_j\rangle, \tag{14}$$

where G_{ij} represent the elements in row i and column j of the Gram matrix. p_i and p_j are the probability distribution of four encoding states. Hence we get

$$G = \frac{1}{8}\begin{pmatrix} A & B \\ B^{\rm T} & C\end{pmatrix}.$$

Here,

$$A = \begin{pmatrix} 1 & a & 0 & 0\\ a & 1 & 0 & 0\\ 0 & 0 & 1 & a\\ 0 & 0 & a & 1\end{pmatrix}, B = \begin{pmatrix} 0 & 0 & b & c\\ 0 & 0 & d & e\\ b & c & 0 & 0\\ d & e & 0 & 0\end{pmatrix},$$

$$C = \begin{pmatrix} 1 & -a & 0 & 0\\ -a & 1 & 0 & 0\\ 0 & 0 & 1 & -a\\ 0 & 0 & -a & 1\end{pmatrix}, \tag{15}$$

with

$$\begin{aligned}a &= \lambda_1 + \lambda_2 - \lambda_3 - \lambda_4,\\ b &= \lambda_1 - \lambda_2 + \lambda_3 - \lambda_4,\\ c &= -\lambda_1 + \lambda_2 + \lambda_3 - \lambda_4 = -d,\\ d &= \lambda_1 - \lambda_2 - \lambda_3 + \lambda_4,\\ e &= -\lambda_1 + \lambda_2 - \lambda_3 + \lambda_4 = -b.\end{aligned} \tag{16}$$

The eigenvalues of our gram matrix are

$$\frac{1}{8}\begin{pmatrix} 1+(a+b+d)\\ 1+(a+b+d)\\ 1+(a-b-d)\\ 1+(a-b-d)\\ 1-(a-b+d)\\ 1-(a-b+d)\\ 1-(a+b-d)\\ 1-(a+b-d)\end{pmatrix}. \tag{17}$$

After simplification, eight eigenvalues can be obtained as $\frac{1}{2}\lambda_1$, $\frac{1}{2}\lambda_1$, $\frac{1}{2}\lambda_2$, $\frac{1}{2}\lambda_2$, $\frac{1}{2}\lambda_3$, $\frac{1}{2}\lambda_3$, $\frac{1}{2}\lambda_4$, $\frac{1}{2}\lambda_4$, respectively. Hence we can obtain

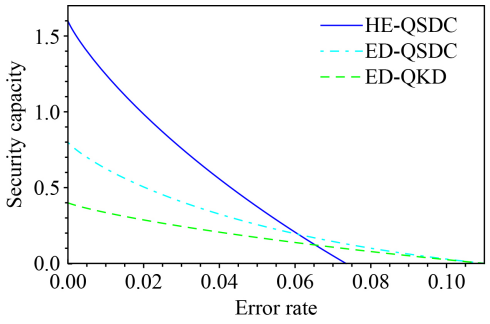

Fig. 3 Comparison of security capacity (bit rate) using Holevo bound (HE-QSDC) and entanglement distillation (ED-QSDC and ED-QKD). For simplicity, we assume that the reception rates of Bob (Q_{B}) and Eve (Q_{E}) are 0.8 and 1, respectively, as it is unlikely for Bob to have a count rate of 1 in practice and the count rate of Eve is not limited. It should be noted that ED-QSDC and ED-QKD do not have a deterministic BSM, so the key rate is multiplied by one half.

$$\begin{aligned} S(\sum_a p_a \rho_{\mathrm{AE},a}) &= S(G) \\ &= h\left(\frac{1}{2}\lambda_1, \frac{1}{2}\lambda_1, \frac{1}{2}\lambda_2, \frac{1}{2}\lambda_2, \frac{1}{2}\lambda_3, \frac{1}{2}\lambda_3, \frac{1}{2}\lambda_4, \frac{1}{2}\lambda_4, \frac{1}{2}\lambda_4, \frac{1}{2}\lambda_4\right) \\ &= 1 + h(\lambda_3+\lambda_4) + (\lambda_1+\lambda_2)h\left(\frac{\lambda_1}{\lambda_1+\lambda_2}\right) \\ &\quad + (\lambda_3+\lambda_4)h\left(\frac{\lambda_3}{\lambda_3+\lambda_4}\right) \leq 1 + h(\epsilon_x) + h(\epsilon_z). \end{aligned} \tag{18}$$

When $d = a * b$, the Von Neumann entropy reaches its maximum value $1+h(\epsilon_x)+h(\epsilon_z)$. Therefore, from Wyner's wiretap channel theory [81], we can get

$$C_s \geq I(A:B) - I(A:E) = 2 - h(e) - h(\epsilon_z) - h(\epsilon_x). \tag{19}$$

When we consider the channel loss, we eventually get

$$C_s \geq Q_{\mathrm{B}}[2 - h(e)] - Q_{\mathrm{E}}[h(\epsilon_z) + h(\epsilon_x)]. \tag{20}$$

Here, e is the error rate of the main channel between Alice and Bob. $h(e)$ is the Shannon entropy. Q_{B} and Q_{E} are reception rates of Bob and Eve, respectively. Usually, Q_{E}=1.

We present a comparison of the security capacities estimated using Holevo bound and entanglement distillation in Fig. 3 [77]. Entanglement distillation is a powerful tool for security analysis that was introduced by Deutsch *et al.* [82], Lo and Chau [83], Shor and Preskill [84]. As for ideal QKD protocol based on entanglement distillation (ED-QKD), the rate is $1 - h(\epsilon_x) - h(\epsilon_z)$, which has been proved in Ref. [83]. To make a reasonable comparison, we uniformly model the quantum channel as a depolarizing channel $\rho \mapsto \frac{pI}{d} + (1-p)\rho$. Here, ρ, p, I and d refer to density matrix, probability, identity matrix and dimensions of quantum states, respectively. In other words, for a d-dimensional quantum system, the depolarizing channel replaces the quantum system with a completely mixed state $\frac{I}{d}$ with probability p and retains the original state with probability $1-p$. Therefore, the error rates of rectilinear basis Z and the diagonal basis X in security check are $\frac{p}{2}$, and the depolarizing probability is $2p - p^2$ after the Bell states pass the depolarizing channel. As the result, the tolerable bit error rate of our protocol is also lower than that of ED-QSDC [77]. From Fig. 3, we can see that our HE-QSDC can encode 1.6 bits of information, resulting in a higher security capacity than ED-QKD at low bit error rates. The error rate threshold of ED-QSDC and ED-QKD is approximately 0.11, while our HE-QSDC is 0.073. This is because our main channel capacity continues to decrease as the bit error rate increases.

5 Fidelities of hybrid entanglement and continuous variables entanglement in lossy environments

In this section, we aim to analyze the fidelities of hybrid entanglement and CV entanglement in a lossy environment. We will now calculate the fidelity of the two methods with an open system. In the case of photon loss, the time evolution of the density matrix of a system can be described using the Born–Markov master equation [85–87]:

$$\frac{\partial \rho}{\partial \tau} = \hat{J}\rho + \hat{L}\rho. \tag{21}$$

Here, τ represents interaction time. $\hat{J}\rho = \gamma \sum_i a_i \rho a_i^\dagger$, $\hat{L}\rho = -\frac{\gamma}{2}\sum_i a_i a_i^\dagger \rho + a_i a_i^\dagger \rho$, where γ, $a_i^\dagger$, and a_i represent decay constant, creation operator and annihilation operator for mode i, respectively. The general solution of Eq. (21) can be described by $\rho(\tau) = \exp[(\hat{J}+\hat{L})\tau]\rho(0)$ [88]. Here, $\rho(0)$ is the initial density operator. In this way, the hybrid entanglement $|\Phi^+\rangle = \frac{1}{\sqrt{2}}(|0_{\mathrm{L}}\rangle|0_{\mathrm{L}}\rangle + |1_{\mathrm{L}}\rangle|1_{\mathrm{L}}\rangle)$ which we used can be expressed as Eq. (22) at time τ [87].

$$\begin{aligned} \rho_1(\tau) = \frac{1}{2}\{&[(t^2|+\rangle\langle+| + r^2|0\rangle\langle 0|) \otimes |t\alpha\rangle\langle t\alpha|]^{\otimes 2} \\ &+ [(t^2|-\rangle\langle-| + r^2|0\rangle\langle 0|) \otimes |-t\alpha\rangle\langle -t\alpha|]^{\otimes 2} \\ &+ (t^2 \mathrm{e}^{-2|\alpha|^2 r^2}|+\rangle\langle-| \otimes |t\alpha\rangle\langle -t\alpha|)^{\otimes 2} \\ &+ (t^2 \mathrm{e}^{-2|\alpha|^2 r^2}|-\rangle\langle+| \otimes |-t\alpha\rangle\langle t\alpha|)^{\otimes 2}\}. \end{aligned} \tag{22}$$

Here, $t = \mathrm{e}^{-\gamma\tau/2}$, $r = \sqrt{1-\mathrm{e}^{-\gamma\tau}}$. The normalization time r is expressed using interaction time τ and decoherence rate γ. Afterwards, we calculate the fidelity of our hybrid entanglement with $F_1 = \langle\Phi^+|\rho_1(\tau)|\Phi^+\rangle$ (see the Appendix for more details) and get

$$F_1 = \frac{1}{4}[2t^4 \mathrm{e}^{-2(1-t)^2|\alpha|^2} + 2t^4 \mathrm{e}^{-|\alpha|^2(4r^2+2(1-t)^2)}]. \tag{23}$$

If we use only CV entanglement in the form of

Eq. (24), we can also calculate the fidelity in a similar manner. Specifically, we can evaluate the fidelity between the original state and the output state by considering the effects of photon loss or other noise on the entangled state

$$|\Phi^+\rangle_{\rm C} = \frac{1}{N_+}(|\alpha\rangle|\alpha\rangle|\alpha\rangle|\alpha\rangle + |-\alpha\rangle|-\alpha\rangle|-\alpha\rangle|-\alpha\rangle). \tag{24}$$

Here, the term $\frac{1}{N_+}$ represents the normalized coefficient, where $N_+ = \sqrt{2+2{\rm e}^{-8\alpha^2}}$. The reason for using $|\Phi^+\rangle_{\rm C}$ in Eq. (24) instead of $|\phi^+\rangle_{\rm C}$ in Eq. (2) is to correspond with hybrid entanglement $|\Phi^+\rangle = \frac{1}{\sqrt{2}}(|0_{\rm L}\rangle|0_{\rm L}\rangle + |1_{\rm L}\rangle|1_{\rm L}\rangle)$. Similarly, we can describe the density matrix of entangled coherent state in Eq. (24) at time τ as follows:

$$\rho_2(\tau) = \frac{1}{N_+^2}\{(|t\alpha\rangle\langle t\alpha|)^{\otimes 4} + (|-t\alpha\rangle\langle -t\alpha|)^{\otimes 4} + {\rm e}^{-8|\alpha|^2 r^2}[(|t\alpha\rangle\langle -t\alpha|)^{\otimes 4} + (|-t\alpha\rangle\langle t\alpha|)^{\otimes 4}]\}. \tag{25}$$

Likewise, we calculate the fidelity of entangled coherent state with $F_2 = {}_{\rm C}\langle\Phi^+|\rho_2(\tau)|\Phi^+\rangle_{\rm C}$ (see the Appendix for more details) and obtain

$$F_2 = [{\rm e}^{-4(1-t)^2|\alpha|^2} + {\rm e}^{-4(1+t)^2|\alpha|^2}] * (2{\rm e}^{-8r^2|\alpha|^2} + 2) + 4{\rm e}^{-2(1-t)^2|\alpha|^2 - 2(1+t)^2|\alpha|^2} * ({\rm e}^{-8r^2|\alpha|^2} + 1). \tag{26}$$

Through numerical simulation, it can be observed that when α is small, such as $\alpha = 1$, the fidelity of direct transmission using entangled coherent states is better compared to that of hybrid entanglement in Fig. 4. However, as α increases, the fidelity of hybrid entanglement gradually surpasses that of entangled coherent states. It is important to note that this difference does not increase with the increase of α. In fact, as α continues to increase, the two curves are approaching each other. This case occurs because as the α increases, the loss also increases, resulting in a rapid decrease in fidelity for both methods in a short period of time.

6 Discussion and conclusion

So far, we outlined the key steps of our protocol and discussed its security. In a practical quantum communication system, both single qubit and coherent state are inevitably affected by noise during the transmission. If a bit-flip error occurs, the initial state $|\Phi_{\rm A}^+\rangle$ may become a mixed state of the form

$$\rho = F|\Phi_{\rm A}^+\rangle\langle\Phi_{\rm A}^+| + (1-F)|\Psi_{\rm A}^+\rangle\langle\Psi_{\rm A}^+|. \tag{27}$$

Here, F and $1-F$ represent the probability of $|\Phi_{\rm A}^+\rangle$ and $|\Psi_{\rm A}^+\rangle$, respectively. On the other hand, in coherent-state transmission, photon loss is a major issue that affects

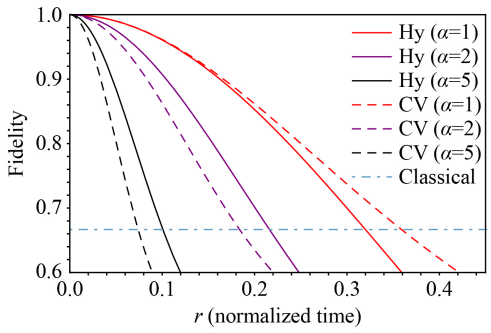

Fig. 4 The fidelity of hybrid entanglement through lossy environment compared with CV entanglement according to different α. Hy ($\alpha = 1$) represents the case of hybrid entanglement when $\alpha = 1$, the same for Hy ($\alpha = 2$) and Hy ($\alpha = 5$). CV ($\alpha = 1$) denotes the case of continuous variables entanglement when $\alpha = 1$, the same for CV ($\alpha = 2$) and CV ($\alpha = 5$). The horizontal dashed lines means the classical limits 2/3. r represents normalization time, which includes interaction time τ and decoherence rate γ. Note that the fidelity of entanglement using CV is higher than that of hybrid entanglement for smaller α (such as $\alpha = 1$). Conversely, for larger α (such as $\alpha = 2$), the fidelity of using hybrid entanglement is higher than that of CV entanglement. As α continues to increase, the fidelity of both entanglements rapidly decreases in a very short time, causing the two curves to continuously converge.

the transmission. Due to the photon loss, a single photon will be successfully transmitted with the transmission efficiency of η, or dissipated into an environment mode with the probability of $1-\eta$ [89, 90]. When we trace over the environment mode, we can see that the photon-loss errors are equivalent to the bit-flip errors in the other basis [91]. Fortunately, entanglement purification of bit-flip errors has been extensively studied for decades [65, 92, 93], and especially the purification of such hybrid entanglement was detailed in Ref. [65]. Moreover, as described in Ref. [73], the photon losses in coherent-state transmission can be incorporated into the mixed state framework with bit-flip error and we can use the same method to purify the photon-loss errors as we do for bit-flip errors.

In QSDC protocols, QM plays an important role [94]. Alice encodes the information after they perform the security check. Therefore, those photons that are not used in security check should be stored in the QM. QM was also exploited to demonstrate QSDC protocol in experiment [32]. In this protocol, we assume that the memory is perfect. Actually, the efficiency and fidelity of QM will also influence the quality of QSDC. Usually, the imperfect part in QM can be regarded as the noise in quantum channel. For example, if the photon is not storied in the QM successfully, it equals to be lost in the quantum channel. In experiment, based on balanced two-channel electromagnetically induced transparency in laser-cooled rubidium atoms, quantum memory for single-photon polarization qubits with an efficiency of >

85% and a fidelity of $> 99\%$ was reported [95]. The fidelity of the qubit in QM can also reach more than 99% with a storage bandwidth of 10 MHz [96]. The coherent storage of light in an atomic frequency comb memory over 1 hour [97]. However, high quality QM for quantum repeater is still a big challenge in existing technology.

In conclusion, we presented the first HE-QSDC protocol. We also perform the security analysis, based on the wiretap channel theory and the Gram matrix method, demonstrates the unconditional security of our HE-QSDC protocol. This protocol has two advantages. First, it employs near-deterministic BSM composed of coherent state and polarized mode in linear optics, which makes the protocol has a higher communication efficiency. Second, when compared to the protocol only using CV entanglement, we have shown that our protocol has higher fidelity when satisfying the large α required for near-deterministic BSM. These advantages make our HE-QSDC protocol become an alternative approach to realize secure communication.

Declarations The authors declare that they have no competing interests and there are no conflicts.

Acknowledgements This work was supported by the National Natural Science Foundation of China (Grant Nos. 11974189, 12175106 and 92365110), the Postgraduate Research & Practice Innovation Program of Jiangsu Province (Grant No. KYCX23-1027), and the Key R&D Program of Guangdong Province (Grant No. 2018B030325002).

Appendix

This Appendix offers a comprehensive analysis of hybrid entanglement in an open system, including the evolution of their density matrix and fidelity over time. The hybrid entanglement $|\Phi^+\rangle = \frac{1}{\sqrt{2}}(|0_{\rm L}\rangle|0_{\rm L}\rangle + |1_{\rm L}\rangle|1_{\rm L}\rangle)$ which we used can be expressed as follows at time τ [87]:

$$\begin{aligned}\rho_1(\tau) = &\frac{1}{2}\{[(t^2|+\rangle\langle+| + r^2|0\rangle\langle 0|) \otimes |t\alpha\rangle\langle t\alpha|]^{\otimes 2}\\ &+ [(t^2|-\rangle\langle-| + r^2|0\rangle\langle 0|) \otimes |-t\alpha\rangle\langle -t\alpha|]^{\otimes 2}\\ &+ (t^2{\rm e}^{-2|\alpha|^2r^2}|+\rangle\langle-| \otimes |t\alpha\rangle\langle -t\alpha|)^{\otimes 2}\\ &+ (t^2{\rm e}^{-2|\alpha|^2r^2}|-\rangle\langle+| \otimes |-t\alpha\rangle\langle t\alpha|)^{\otimes 2}\}\\ = &\frac{1}{2}\{[(t^4|+\rangle|+\rangle\langle+|\langle+| + r^4|0\rangle|0\rangle\langle 0|\langle 0|\\ &+ t^2r^2(|+\rangle|0\rangle\langle 0|\langle+| + |0\rangle|+\rangle\langle+|\langle 0|)]\\ &\otimes |t\alpha\rangle|t\alpha\rangle\langle t\alpha|\langle t\alpha|\\ &+ [(t^4|-\rangle|-\rangle\langle-|\langle-| + r^4|0\rangle|0\rangle\langle 0|\langle 0|\\ &+ t^2r^2(|-\rangle|0\rangle\langle 0|\langle-| + |0\rangle|-\rangle\langle-|\langle 0|)]\\ &\otimes |-t\alpha\rangle|-t\alpha\rangle\langle -t\alpha|\langle -t\alpha|\\ &+ t^4{\rm e}^{-4|\alpha|^2r^2}(|+\rangle|+\rangle\langle-|\langle-| \otimes |t\alpha\rangle|t\alpha\rangle\langle -t\alpha|\langle -t\alpha|\\ &+ |-\rangle|-\rangle\langle+|\langle+| \otimes |-t\alpha\rangle|-t\alpha\rangle\langle t\alpha|\langle t\alpha|)\}.\end{aligned} \tag{A1}$$

Therefore, the fidelity of the hybrid entanglement at time τ can be represented as

$$\begin{aligned}F_1 = &\langle\Phi^+|\rho_1(\tau)|\Phi^+\rangle\\ = &\frac{1}{4}[(\langle 0_{\rm L}|\langle 0_{\rm L}| + \langle 1_{\rm L}|\langle 1_{\rm L}|) \otimes \rho_1(\tau)\\ &\otimes (|0_{\rm L}\rangle|0_{\rm L}\rangle + |1_{\rm L}\rangle|1_{\rm L}\rangle)\}\\ = &\frac{1}{4}\{(\langle+|\langle+|\langle\alpha\langle\alpha| + (\langle-|\langle-|\langle-\alpha\langle-\alpha|) \otimes \rho_1(\tau)\\ &\otimes\ (|+\rangle|+\rangle|\alpha\rangle|\alpha\rangle + |-\rangle|-\rangle|-\alpha\rangle|-\alpha\rangle)].\end{aligned} \tag{A2}$$

The above equation can be detailed as

$$\begin{aligned}&\langle+|\langle+|\langle\alpha|\langle\alpha|\rho_1(\tau)|+\rangle|+\rangle|\alpha\rangle|\alpha\rangle = t^4{\rm e}^{-2(1-t)^2|\alpha|^2},\\ &\langle+|\langle+|\langle\alpha|\langle\alpha|\rho_1(\tau)|-\rangle|-\rangle|\alpha\rangle|\alpha\rangle = t^4{\rm e}^{-4|\alpha|^2r^2-2(1-t)^2|\alpha|^2},\\ &\langle-|\langle-|\langle\alpha|\langle\alpha|\rho_1(\tau)|+\rangle|+\rangle|\alpha\rangle|\alpha\rangle = t^4{\rm e}^{-4|\alpha|^2r^2-2(1-t)^2|\alpha|^2},\\ &\langle-|\langle-|\langle\alpha|\langle\alpha|\rho_1(\tau)|-\rangle|-\rangle|\alpha\rangle|\alpha\rangle = t^4{\rm e}^{-2(1-t)^2|\alpha|^2}.\end{aligned} \tag{A3}$$

Here we will use the inner product of coherent states, which can be represented as

$$\begin{aligned}&\langle\alpha|t\alpha\rangle = {\rm e}^{-\frac{1}{2}(1-t)^2\alpha^2} = \langle t\alpha|\alpha\rangle,\\ &\langle -t\alpha|-\alpha\rangle = {\rm e}^{-\frac{1}{2}(1-t)^2\alpha^2} = \langle -t\alpha|-\alpha\rangle.\end{aligned} \tag{A4}$$

By summing up the four terms in Eq. (A3), we can obtain the fidelity of the hybrid entanglement at time τ in an open system as

$$F_1 = \frac{1}{4}(2t^4{\rm e}^{-2(1-t)^2|\alpha|^2} + 2t^4{\rm e}^{-4|\alpha|^2r^2-2(1-t)^2|\alpha|^2}). \tag{A5}$$

Afterwards, we will analyze the fidelity of CV entanglement in Eq. (24) at time τ in an open system. We can employ $\exp[(\hat{J}+\hat{L})\tau]|\alpha\rangle\langle\beta| = \langle\beta|\alpha\rangle^{1-t^2}|\alpha t\rangle\langle\beta t|$ in Ref. [76] to Eq. (24) and we can get

$$\begin{aligned}\rho_2(\tau) = &\frac{1}{N_+^2}\{(|t\alpha\rangle\langle t\alpha|)^{\otimes 4} + (|-t\alpha\rangle\langle -t\alpha|)^{\otimes 4}\\ &+ {\rm e}^{-8|\alpha|^2r^2}[(|t\alpha\rangle\langle -t\alpha|)^{\otimes 4} + (|-t\alpha\rangle\langle t\alpha|)^{\otimes 4}]\}.\end{aligned} \tag{A6}$$

Therefore, the fidelity of CV entanglement at time τ can be expressed as

$$\begin{aligned}F_1 = &{}_C\langle\Phi^+|\rho_2(\tau)|\Phi^+\rangle_C\\ = &\frac{1}{N_+^4}[(\langle\alpha|\langle\alpha|\langle\alpha|\langle\alpha| + \langle-\alpha|\langle-\alpha|\langle-\alpha|\langle-\alpha|) \otimes \rho_2(\tau)\\ &\otimes (|\alpha\rangle|\alpha\rangle|\alpha\rangle|\alpha\rangle + |-\alpha\rangle|-\alpha\rangle|-\alpha\rangle|-\alpha\rangle)].\end{aligned} \tag{A7}$$

Similarly, we calculate the four parts by decomposing Eq. (A7):

$$
\begin{aligned}
&\langle\alpha|\langle\alpha|\langle\alpha|\langle\alpha|\rho_2(\tau)|\alpha\rangle|\alpha\rangle|\alpha\rangle|\alpha\rangle \\
&\quad = \mathrm{e}^{-4(1-t)^2|\alpha|^2} + \mathrm{e}^{-4(1+t)^2|\alpha|^2} + 2\mathrm{e}^{-8|\alpha|^2 r^2} \\
&\qquad \cdot \mathrm{e}^{-2(1-t)^2|\alpha|^2 - 2(1+t)^2|\alpha|^2}, \\
&\langle\alpha|\langle\alpha|\langle\alpha|\langle\alpha|\rho_2(\tau)|-\alpha\rangle|-\alpha\rangle|-\alpha\rangle|-\alpha\rangle \\
&\quad = 2\mathrm{e}^{-2(1-t)^2|\alpha|^2 - 2(1+t)^2|\alpha|^2} + \mathrm{e}^{-8|\alpha|^2 r^2} \\
&\qquad \cdot [\mathrm{e}^{-4(1-t)^2|\alpha|^2} + \mathrm{e}^{-4(1+t)^2|\alpha|^2}], \\
&\langle-\alpha|\langle-\alpha|\langle-\alpha|\langle-\alpha|\rho_2(\tau)|\alpha\rangle|\alpha\rangle|\alpha\rangle|\alpha\rangle \\
&\quad = 2\mathrm{e}^{-2(1-t)^2|\alpha|^2 - 2(1+t)^2|\alpha|^2} + \mathrm{e}^{-8|\alpha|^2 r^2} \\
&\qquad \cdot [\mathrm{e}^{-4(1-t)^2|\alpha|^2} + \mathrm{e}^{-4(1+t)^2|\alpha|^2}], \\
&\langle-\alpha|\langle-\alpha|\langle-\alpha|\langle-\alpha|\rho_2(\tau)|-\alpha\rangle|-\alpha\rangle|-\alpha\rangle|-\alpha\rangle \\
&\quad = \mathrm{e}^{-4(1-t)^2|\alpha|^2} + \mathrm{e}^{-4(1+t)^2|\alpha|^2} + 2\mathrm{e}^{-8|\alpha|^2 r^2} \\
&\qquad \cdot \mathrm{e}^{-2(1-t)^2|\alpha|^2 - 2(1+t)^2|\alpha|^2}. \qquad \text{(A8)}
\end{aligned}
$$

Finally, by summing up the four terms in Eq. (A8), we can obtain the fidelity of the CV entanglement at time τ in an open system as

$$
\begin{aligned}
F_2 = &[\mathrm{e}^{-4(1-t)^2|\alpha|^2} + \mathrm{e}^{-4(1+t)^2|\alpha|^2}] * (2\mathrm{e}^{-8r^2|\alpha|^2} + 2) \\
&+ 4\mathrm{e}^{-2(1-t)^2|\alpha|^2 - 2(1+t)^2|\alpha|^2} * (\mathrm{e}^{-8r^2|\alpha|^2} + 1). \qquad \text{(A9)}
\end{aligned}
$$

References

1. V. Scarani, H. Bechmann-Pasquinucci, N. J. Cerf, M. Dušek, N. Lütkenhaus, and M. Peev, The security of practical quantum key distribution, *Rev. Mod. Phys.* 81(3), 1301 (2009)
2. F. H. Xu, X. F. Ma, Q. Zhang, H. K. Lo, and J. W. Pan, Secure quantum key distribution with realistic devices, *Rev. Mod. Phys.* 92(2), 025002 (2020)
3. A. K. Ekert, Quantum cryptography based on Bell's theorem, *Phys. Rev. Lett.* 67(6), 661 (1991)
4. X. F. Ma, B. Qi, Y. Zhao, and H. K. Lo, Practical decoy state for quantum key distribution, *Phys. Rev. A* 72(1), 012326 (2005)
5. X. Ma, C. H. F. Fung, and H. K. Lo, Quantum key distribution with entangled photon sources, *Phys. Rev. A* 76(1), 012307 (2007)
6. X. L. Su, Applying Gaussian quantum discord to quantum key distribution, *Chin. Sci. Bull.* 59(11), 1083 (2014)
7. M. Hillery, V. Bužek, and A. Berthiaume, Quantum secret sharing, *Phys. Rev. A* 59(3), 1829 (1999)
8. A. Shen, X. Y. Cao, Y. Wang, Y. Fu, J. Gu, W. B. Liu, C. X. Weng, H. L. Yin, and Z. B. Chen, Experimental quantum secret sharing based on phase encoding of coherent states, *Sci. China Phys. Mech. Astron.* 66(6), 260311 (2023)
9. G. L. Long and X. S. Liu, Theoretically efficient high-capacity quantum-key-distribution scheme, *Phys. Rev. A* 65(3), 032302 (2002)
10. F. G. Deng, G. L. Long, and X. S. Liu, Two-step quantum direct communication protocol using the Einstein–Podolsky–Rosen pair block, *Phys. Rev. A* 68(4), 042317 (2003)
11. F. G. Deng and G. L. Long, Secure direct communication with a quantum one-time pad, *Phys. Rev. A* 69(5), 052319 (2004)
12. P. H. Niu, Z. R. Zhou, Z. S. Lin, Y. B. Sheng, L. G. Yin, and G. L. Long, Measurement-device-independent quantum communication without encryption, *Sci. Bull. (Beijing)* 63(20), 1345 (2018)
13. Z. R. Zhou, Y. B. Sheng, P. H. Niu, L. G. Yin, G. L. Long, and L. Hanzo, Measurement-device-independent quantum secure direct communication, *Sci. China Phys. Mech. Astron.* 63(3), 230362 (2020)
14. L. Zhou, Y. B. Sheng, and G. L. Long, Device-independent quantum secure direct communication against collective attacks, *Sci. Bull. (Beijing)* 65(1), 12 (2020)
15. L. Zhou, B. W. Xu, W. Zhong, and Y. B. Sheng, Device-independent quantum secure direct communication with single-photon sources, *Phys. Rev. Appl.* 19(1), 014036 (2023)
16. H. Zeng, M. M. Du, W. Zhong, L. Zhou, and Y. B. Sheng, High-capacity device-independent quantum secure direct communication based on hyper-encoding, *Fundament. Res.*, doi: 10.1016/j.fmre.2023.11.006 (2023)
17. Y. B. Sheng, L. Zhou, and G. L. Long, One-step quantum secure direct communication, *Sci. Bull. (Beijing)* 67(4), 367 (2022)
18. L. Zhou and Y. B. Sheng, One-step device-independent quantum secure direct communication, *Sci. China Phys. Mech. Astron.* 65(5), 250311 (2022)
19. J. W. Ying, L. Zhou, W. Zhong, and Y. B. Sheng, Measurement-device-independent one-step quantum secure direct communication, *Chin. Phys. B* 31(12), 120303 (2022)
20. X. R. Jin, X. Ji, Y. Q. Zhang, S. Zhang, S. K. Hong, K. H. Yeon, and C. I. Um, Three-party quantum secure direct communication based on GHZ states, *Phys. Lett. A* 354(1–2), 67 (2006)
21. Q. Zhang, M. M. Du, W. Zhong, Y. B. Sheng, and L. Zhou, Single-photon based three-party quantum secure direct communication with identity authentication, *Ann. Phys. (Berlin)*, doi: 10.1002/andp.202300407 (2023)
22. Y. P. Hong, L. Zhou, W. Zhong, and Y. B. Sheng, Measurement-device-independent three-party quantum secure direct communication, *Quantum Inform. Process.* 22(2), 111 (2023)
23. Y. X. Xiao, L. Zhou, W. Zhong, M. M. Du, and Y. B. Sheng, The hyperentanglement-based quantum secure direct communication protocol with single-photon measurement, *Quantum Inform. Process.* 22(9), 339 (2023)
24. A. D. Zhu, Y. Xia, Q. B. Fan, and S. Zhang, Secure direct communication based on secret transmitting order of particles, *Phys. Rev. A* 73(2), 022338 (2006)
25. Z. W. Cao, L. Wang, K. X. Liang, G. Chai, and J. Y. Peng, Continuous-variable quantum secure direct communication based on Gaussian mapping, *Phys. Rev. Appl.* 16(2), 024012 (2021)
26. Z. W. Cao, Y. Lu, G. Chai, H. Yu, K. X. Liang, and L. Wang, Realization of quantum secure direct communication with continuous variable, *Research* 6, 0193 (2023)
27. S. Srikara, K. Thapliyal, and A. Pathak, Continuous

variable direct secure quantum communication using Gaussian states, *Quantum Inform. Process.* 19(4), 132 (2020)
28. K. X. Liang, Z. W. Cao, X. L. Chen, L. Wang, G. Chai, and J. Y. Peng, A quantum secure direct communication scheme based on intermediate-basis, *Front. Phys.* 18(5), 51301 (2023)
29. T. Li and G. L. Long, Quantum secure direct communication based on single-photon Bell-state measurement, *New J. Phys.* 22(6), 063017 (2020)
30. Z. D. Ye, D. Pan, Z. Sun, C. G. Du, L. G. Yin, and G. L. Long, Generic security analysis framework for quantum secure direct communication, *Front. Phys.* 16(2), 21503 (2021)
31. J. Y. Hu, B. Yu, M. Y. Jing, L. T. Xiao, S. T. Jia, G. Q. Qin, and G. L. Long, Experimental quantum secure direct communication with single photons, *Light Sci. Appl.* 5(9), e16144 (2016)
32. W. Zhang, D. S. Ding, Y. B. Sheng, L. Zhou, B. S. Shi, and G. C. Guo, Quantum secure direct communication with quantum memory, *Phys. Rev. Lett.* 118(22), 220501 (2017)
33. F. Zhu, W. Zhang, Y. B. Sheng, and Y. D. Huang, Experimental long-distance quantum secure direct communication, *Sci. Bull. (Beijing)* 62(22), 1519 (2017)
34. D. Pan, Z. S. Lin, J. W. Wu, H. R. Zhang, Z. Sun, D. Ruan, L. G. Yin, and G. L. Long, Experimental free-space quantum secure direct communication and its security analysis, *Photon. Res.* 8(9), 1522 (2020)
35. Z. Qi, Y. Li, Y. W. Huang, J. Feng, Y. L. Zheng, and X. F. Chen, A 15-user quantum secure direct communication network, *Light Sci. Appl.* 10(1), 183 (2021)
36. X. Liu, D. Luo, G. L. Lin, Z. H. Chen, C. F. Huang, S. Z. Li, C. X. Zhang, Z. R. Zhang, and K. J. Wei, Fiber-based quantum secure direct communication without active polarization compensation, *Sci. China Phys. Mech. Astron.* 65(12), 120311 (2022)
37. H. Zhang, Z. Sun, R. Qi, L. Yin, G. L. Long, and J. Lu, Realization of quantum secure direct communication over 100 km fiber with time-bin and phase quantum states, *Light Sci. Appl.* 11(1), 83 (2022)
38. I. Paparelle, F. Mousavi, F. Scazza, A. Bassi, M. Paris, and A. Zavatta, Practical quantum secure direct communication with squeezed states, arXiv: 2306.14322 (2023)
39. Y. Fu, H. L. Yin, T. Y. Chen, and Z. B. Chen, Long-distance measurement-device-independent multi-party quantum communication, *Phys. Rev. Lett.* 114(9), 090501 (2015)
40. T. Pramanik, D. H. Lee, Y. W. Cho, H. Lim, S. Han, H. Jung, S. Moon, K. J. Lee, and Y. Kim, Equitable multiparty quantum communication without a trusted third party, *Phys. Rev. Appl.* 14(6), 064074 (2020)
41. S. M. Lee, S. W. Lee, H. Jeong, and H. S. Park, Quantum teleportation of shared quantum secret, *Phys. Rev. Lett.* 124(6), 060501 (2020)
42. A. Muller, J. Breguet, and N. Gisin, Experimental demonstration of quantum cryptography using polarized photons in optical fiber over more than 1 km, *Europhys. Lett.* 23(6), 383 (1993)
43. P. D. Townsend and I. A. Thompson, A quantum key distribution channel based on optical fibre, *J. Mod. Opt.* 41(12), 2425 (1994)
44. H. K. Lo, M. Curty, and B. Qi, Measurement-device-independent quantum key distribution, *Phys. Rev. Lett.* 108(13), 130503 (2012)
45. F. Grosshans, G. Van Assche, J. Wenger, R. Brouri, N. J. Cerf, and P. Grangier, Quantum key distribution using Gaussian-modulated coherent states, *Nature* 421(6920), 238 (2003)
46. J. Lodewyck, M. Bloch, R. García-Patrón, S. Fossier, E. Karpov, E. Diamanti, T. Debuisschert, N. J. Cerf, R. Tualle-Brouri, S. W. McLaughlin, and P. Grangier, Quantum key distribution over 25 km with an all-fiber continuous-variable system, *Phys. Rev. A* 76(4), 042305 (2007)
47. C. Wang, D. Huang, P. Huang, D. Lin, J. Peng, and G. Zeng, 25 MHz clock continuous-variable quantum key distribution system over 50 km fiber channel, *Sci. Rep.* 5(1), 14607 (2015)
48. Y. Zhang, Z. Chen, S. Pirandola, X. Wang, C. Zhou, B. Chu, Y. Zhao, B. Xu, S. Yu, and H. Guo, Long-distance continuous-variable quantum key distribution over 202.81 km of fiber, *Phys. Rev. Lett.* 125(1), 010502 (2020)
49. J. B. Brask, I. Rigas, E. S. Polzik, U. L. Andersen, and A. S. Sørensen, Hybrid long-distance entanglement distribution protocol, *Phys. Rev. Lett.* 105(16), 160501 (2010)
50. P. van Loock, Optical hybrid approaches to quantum information, *Laser Photonics Rev.* 5(2), 167 (2011)
51. S. W. Lee and H. Jeong, Near-deterministic quantum teleportation and resource-efficient quantum computation using linear optics and hybrid qubits, *Phys. Rev. A* 87(2), 022326 (2013)
52. S. Bose and H. Jeong, Quantum teleportation of hybrid qubits and single-photon qubits using Gaussian resources, *Phys. Rev. A* 105(3), 032434 (2022)
53. J. W. Pan, M. Daniell, S. Gasparoni, G. Weihs, and A. Zeilinger, Experimental demonstration of four-photon entanglement and high-fidelity teleportation, *Phys. Rev. Lett.* 86(20), 4435 (2001)
54. J. Calsamiglia and N. Lütkenhaus, Maximum efficiency of a linear-optical Bell-state analyzer, *Appl. Phys. B* 72(1), 67 (2001)
55. F. Grosshans and P. Grangier, Continuous variable quantum cryptography using coherent states, *Phys. Rev. Lett.* 88(5), 057902 (2002)
56. A. Ourjoumtsev, H. Jeong, R. Tualle-Brouri, and P. Grangier, Generation of optical "Schrödinger cats" from photon number states, *Nature* 448(7155), 784 (2007)
57. B. H. Li, Y. M. Xie, Z. Li, C. X. Weng, C. L. Li, H. L. Yin, and Z. B. Chen, Long-distance twin-field quantum key distribution with entangled sources, *Opt. Lett.* 46(22), 5529 (2021)
58. Y. M. Xie, B. H. Li, Y. S. Lu, X. Y. Cao, W. B. Liu, H. L. Yin, and Z. B. Chen, Overcoming the rate-distance limit of device-independent quantum key distribution, *Opt. Lett.* 46(7), 1632 (2021)
59. S. L. Braunstein and P. van Loock, Quantum information with continuous variables, *Rev. Mod. Phys.* 77(2), 513 (2005)

60. H. Jeong, A. Zavatta, M. Kang, S. W. Lee, L. S. Costanzo, S. Grandi, T. C. Ralph, and M. Bellini, Generation of hybrid entanglement of light, *Nat. Photonics* 8(7), 564 (2014)
61. O. Morin, K. Huang, J. Liu, H. Le Jeannic, C. Fabre, and J. Laurat, Remote creation of hybrid entanglement between particle-like and wave-like optical qubits, *Nat. Photonics* 8(7), 570 (2014)
62. H. Kwon and H. Jeong, Generation of hybrid entanglement between a single-photon polarization qubit and a coherent state, *Phys. Rev. A* 91(1), 012340 (2015)
63. J. H. Shapiro, Single-photon Kerr nonlinearities do not help quantum computation, *Phys. Rev. A* 73(6), 062305 (2006)
64. J. H. Shapiro and M. Razavi, Continuous-time cross-phase modulation and quantum computation, *New J. Phys.* 9(1), 16 (2007)
65. C. C. Luo, L. Zhou, W. Zhong, and Y. B. Sheng, Purification for hybrid logical qubit entanglement, *Quantum Inform. Process.* 21(8), 300 (2022)
66. P. van Loock, T. D. Ladd, K. Sanaka, F. Yamaguchi, K. Nemoto, W. J. Munro, and Y. Yamamoto, Hybrid quantum repeater using bright coherent light, *Phys. Rev. Lett.* 96(24), 240501 (2006)
67. M. Bergmann and P. van Loock, Hybrid quantum repeater for qudits, *Phys. Rev. A* 99(3), 032349 (2019)
68. M. Fujiwara, M. Toyoshima, M. Sasaki, K. Yoshino, Y. Nambu, and A. Tomita, Performance of hybrid entanglement photon pair source for quantum key distribution, *Appl. Phys. Lett.* 95(26), 261103 (2009)
69. M. Fujiwara, K. Yoshino, Y. Nambu, T. Yamashita, S. Miki, H. Terai, Z. Wang, M. Toyoshima, A. Tomita, and M. Sasaki, Modified E91 protocol demonstration with hybrid entanglement photon source, *Opt. Express* 22(11), 13616 (2014)
70. C. X. Zhang, B. H. Guo, G. M. Cheng, J. J. Guo, and R. H. Fan, Spin–orbit hybrid entanglement quantum key distribution scheme, *Sci. China Phys. Mech. Astron.* 57(11), 2043 (2014)
71. S. L. Zhang, Improving long-distance distribution of entangled coherent state with the method of twin-field quantum key distribution, *Opt. Express* 27(25), 37087 (2019)
72. S. Bose, J. Singh, A. Cabello, and H. Jeong, Long distance measurement-device-independent quantum key distribution using entangled states between continuous and discrete variables, arXiv: 2305.18906 (2023)
73. Y. B. Sheng, L. Zhou, and G. L. Long, Hybrid entanglement purification for quantum repeaters, *Phys. Rev. A* 88(2), 022302 (2013)
74. H. Jeong and M. S. Kim, Efficient quantum computation using coherent states, *Phys. Rev. A* 65(4), 042305 (2002)
75. D. V. Sychev, A. E. Ulanov, E. S. Tiunov, A. A. Pushkina, A. Kuzhamuratov, V. Novikov, and A. I. Lvovsky, Entanglement and teleportation between polarization and wave-like encodings of an optical qubit, *Nat. Commun.* 9(1), 3672 (2018)
76. H. Jeong, M. S. Kim, and J. Lee, Quantum-information processing for a coherent superposition state via a mixed entangled coherent channel, *Phys. Rev. A* 64(5), 052308 (2001)
77. J. W. Wu, Z. S. Lin, L. G. Yin, and G. L. Long, Security of quantum secure direct communication based on Wyner's wiretap channel theory, *Quantum Eng.* 1(4), e26 (2019)
78. R. Y. Qi, Z. Sun, Z. S. Lin, P. H. Niu, W. T. Hao, L. Y. Song, Q. Huang, J. C. Gao, L. G. Yin, and G. L. Long, Implementation and security analysis of practical quantum secure direct communication, *Light Sci. Appl.* 8(1), 22 (2019)
79. A. S. Holevo, Bounds for the quantity of information transmitted by a quantum communication channel, *Probl. Peredachi Inf.* 9(3), 177 (1973)
80. R. Jozsa and J. Schlienz, Distinguishability of states and von Neumann entropy, *Phys. Rev. A* 62(1), 012301 (2000)
81. A. D. Wyner, The wire-tap channel, *Bell Syst. Tech. J.* 54(8), 1355 (1975)
82. D. Deutsch, A. Ekert, R. Jozsa, C. Macchiavello, S. Popescu, and A. Sanpera, Quantum privacy amplification and the security of quantum cryptography over noisy channels, *Phys. Rev. Lett.* 77(13), 2818 (1996)
83. H. K. Lo and H. F. Chau, Unconditional security of quantum key distribution over arbitrarily long distances, *Science* 283(5410), 2050 (1999)
84. P. W. Shor and J. Preskill, Simple proof of security of the BB84 quantum key distribution protocol, *Phys. Rev. Lett.* 85(2), 441 (2000)
85. W. H. Louisell, Quantum Statistical Properties of Radiation, New York: Wiley, 1973
86. H. Kim, J. Park, and H. Jeong, Transfer of different types of optical qubits over a lossy environment, *Phys. Rev. A* 89(4), 042303 (2014)
87. H. Kim, S. W. Lee, and H. Jeong, Two different types of optical hybrid qubits for teleportation in a lossy environment, *Quantum Inform. Process.* 15(11), 4729 (2016)
88. S. J. D. Phoenix, Wave-packet evolution in the damped oscillator, *Phys. Rev. A* 41(9), 5132 (1990)
89. S. J. van Enk and O. Hirota, Entangled coherent states: Teleportation and decoherence, *Phys. Rev. A* 64(2), 022313 (2001)
90. T. C. Ralph, A. Gilchrist, G. J. Milburn, W. J. Munro, and S. Glancy, Quantum computation with optical coherent states, *Phys. Rev. A* 68(4), 042319 (2003)
91. P. van Loock, N. Lütkenhaus, W. J. Munro, and K. Nemoto, Quantum repeaters using coherent-state communication, *Phys. Rev. A* 78(6), 062319 (2008)
92. C. H. Bennett, G. Brassard, S. Popescu, B. Schumacher, J. A. Smolin, and W. K. Wootters, Purification of noisy entanglement and faithful teleportation via noisy channels, *Phys. Rev. Lett.* 76(5), 722 (1996)
93. P. S. Yan, L. Zhou, W. Zhong, and Y. B. Sheng, Advances in quantum entanglement purification, *Sci. China Phys. Mech. Astron.* 66(5), 250301 (2023)
94. Z. Q. Zhou, C. Liu, C. F. Li, G. C. Guo, D. Oblak, M. Lei, A. Faraon, M. Mazzera, and H. de Riedmatten, Photonic integrated quantum memory in rare-earth doped solids, *Laser Photonics Rev.* 17(10), 2300257 (2023)

95. Y. F. Wang, J. F. Li, S. C. Zhang, K. Y. Su, Y. R. Zhou, K. Y. Liao, S. W. Du, H. Yan, and S. L. Zhu, Efficient quantum memory for single-photon polarization qubits, *Nat. Photonics* 13(5), 346 (2019)
96. T. X. Zhu, C. Liu, M. Jin, M. X. Su, Y. P. Liu, W. J. Li, Y. Ye, Z. Q. Zhou, C. F. Li, and G. C. Guo, On-demand integrated quantum memory for polarization qubits, *Phys. Rev. Lett.* 128(18), 180501 (2022)
97. Y. Ma, Y. Z. Ma, Z. Q. Zhou, C. F. Li, and G. C. Guo, One-hour coherent optical storage in an atomic frequency comb memory, *Nat. Commun.* 12(1), 2381 (2021)